Journal of
Mechanics of
Materials and Structures

METAL SANDWICH PLATES WITH POLYMER FOAM-FILLED CORES

A. Vaziri, Z. Xue and J. W. Hutchinson

Volume 1, Nº 1 January 2006

mathematical sciences publishers

JOURNAL OF MECHANICS OF MATERIALS AND STRUCTURES
Vol. 1, No. 1, 2006

METAL SANDWICH PLATES WITH POLYMER FOAM-FILLED CORES

A. VAZIRI, Z. XUE AND J. W. HUTCHINSON

The role of low-density structural polymeric foams filling the interstices of the cores of metal sandwich plates is studied to ascertain the strengthening of the cores and the enhancement of plate performance under crushing and impulsive loads. Square honeycomb and folded plate steel cores filled with two densities of structural foams are studied. The foam makes direct contributions to core strength and stiffness, but its main contribution is in supplying lateral support to core members thereby enhancing the buckling strength of these members. Performance is assessed at fixed total weight of the sandwich plate such that the weight of the foam is traded against that of the metal. The outcome of the comparative study suggests that plates with foam-filled cores can perform as well, or nearly as well, as plates of the same weight with unfilled cores. The decision on use of foams in the cores is therefore likely to rest on multifunctional advantages such as acoustic and thermal insulation or environmental isolation of core interstices.

1. Introduction

Polymeric foams offer unique structural, thermal and acoustic properties, which make them an excellent choice for many engineering applications [Gibson and Ashby 1997]. Here, we explore another possible application of structural foams: as a filler of the interstices of the cores of metal sandwich plates designed to withstand intense pressure pulses. The main purpose of the filler would be to stabilize core members against buckling, increasing the effective strength of the core. To assess whether structural foam is effective in this application, behaviors of sandwich plates with and without filler, but constrained to have the same total weight, are compared for localized three-point bending loads and for clamped plates subject to uniformly distributed pressure pulses. Attention is directed to two classes of cores: square honeycombs and folded plates (Figure 1).

The background to the present study is the recent discovery that metal sandwich plates can be designed to sustain smaller deflections than monolithic solid

Keywords: polymeric foams, sandwich plates, honeycomb cores, folded plate cores, impulsive loads.

Corresponding author: J. W. Hutchinson.

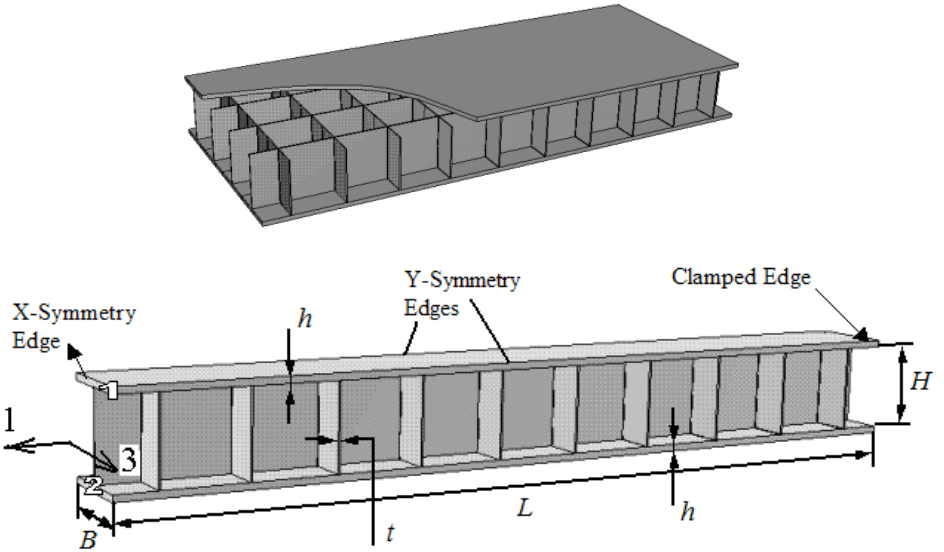

(a) square honeycomb sandwich plate

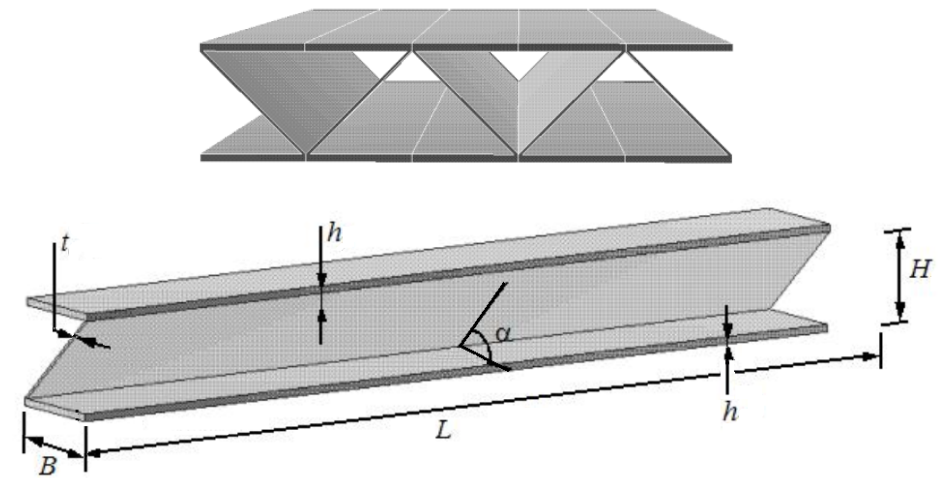

(b) folded sandwich plate

Figure 1: Schematic diagram of sandwich plate core configuration and corresponding computation model of sandwich panel (the polymeric foam components are not shown)

plates of the same weight when subject to intense pressure pulses, particularly when the pulse is transmitted through water [Xue and Hutchinson 2003; Xue and Hutchinson 2004a; Xue and Hutchinson 2004b; Hutchinson and Xue 2005]. The core plays a critical role in the performance of the sandwich plate: typically, it must be able to absorb more than one half of the initial kinetic energy imparted to the plate by crushing in the early stages of deformation prior to significant overall bending and stretching without unduly reducing the separation between the face sheets. High crushing strength and energy absorption per unit mass of the core is therefore important. Square honeycomb cores have been shown to be especially effective [Xue and Hutchinson 2004a], and this is one of the core-types considered here. Folded plate cores are more susceptible to buckling under crushing than square honeycombs but are nevertheless effective, and they have manufacturing advantages. In this paper, enhancement of the buckling resistance of the core webs due to lateral support of the foam will be investigated. The tradeoff against such enhancement is the inevitable loss in bending and/or stretching strength accompanying the reduction in metal required to pay for the weight of the foam. The net gain or loss to the overall performance of the plate by incorporating the foam is by no means obvious when the total mass of the plate is constrained to be constant.

The paper begins with the specification of the sandwich plate geometries and material properties in Section 2. The material comprising the sandwich plate core and face sheet is stainless steel (#304). The foam material is a closed-cell PVC foam material with the commercial name *Divinycell*. Two commercially available densities of this polymeric foam are considered, H100 and H200. Details of the continuum constitutive model of the polymeric foam materials are described in Section 2.1. The finite element modeling is described in Section 2.2. A limited investigation of the response of the core to three basic stressing histories (crushing, shear and stretching) is conducted in Section 3 to provide insight into the effect of filling the core interstices with foam. Section 4 presents comparative results, with and without the foam, for wide sandwich plates clamped along opposite edges and subject to a quasi-static load applied by an indenter. Corresponding results for clamped plates subject to a uniformly distributed intense impulse are given in Section 5. Limited results for the plastic energy dissipation history of each component of the empty and foam-filled sandwich plates under impulsive load are presented in Section 6. Conclusions are drawn in Section 7, where topics for further research will also be noted.

2. Specification of sandwich plates and material properties

2.1. ***Sandwich plates.*** Infinite sandwich plates of width $2L$ that are clamped along their edges are considered. Figure 1 shows the periodic units employed in the finite

element models of the sandwich plate (the foam is not depicted). Both types of sandwich plates have core height H, core web thickness t, and face sheet thickness h. The square honeycomb core has web spacing B. The folded plate core has an inclination angle α.

Denote the densities of the steel and foam by ρ_s and ρ_f, respectively. The average density of the core, $\bar{\rho}_c$, is

$$\bar{\rho}_c = \upsilon_s \rho_s + \rho_f (1 - \upsilon_s) \tag{1}$$

where υ_s is the volume fraction of the core occupied by steel. Full-scale metal sandwich plates designed to be effective against impulsive loads have cores with a low volume fraction of material, typically with υ_s less than 0.05 [Xue and Hutchinson 2004a]. The mass per area of the sandwich plate, M, including the mass of the foam, is given by

$$M = (2\rho_s h + \bar{\rho}_c H) \tag{2}$$

For the *square honeycomb core:*

$$\upsilon_s = 2\frac{t}{B} - \left(\frac{t}{B}\right)^2 \cong 2\frac{t}{B} \tag{3}$$

With L, M, ρ_s and ρ_f specified, the geometry of the square honey plate is fully determined by the three independent parameters υ_s, H/L and B/L. The trade-off of steel against foam due to filling the interstices of the core with foam when the mass of the core is held fixed can be seen in Figure 2. In that plot, $H_s \equiv \bar{\rho}_c H/\rho_s$ is the thickness of a solid steel sheet with the same mass/area as the core. The volume fraction of steel in the core as a function of H/H_s, $\upsilon_s = (H/H_s - \rho_f/\rho_s)/(1 - \rho_f/\rho_s)$, is shown for the empty core ($\rho_f = 0$) and for the density ratios considered in this paper: H100 ($\rho_f/\rho_s = 0.0125$) and H200 ($\rho_f/\rho_s = 0.025$). For the full-scale plates considered in this paper, typically, $H/H_s \cong 25$ such that the empty core has $\upsilon_s \cong 0.04$, while the equal weight core filled with H200 foam has only about half the amount of steel. Of course, steel can be traded from the face sheets as well as from the core.

For the *folded sandwich core:*

$$\upsilon_s = \frac{t/H}{t/H + \cos\alpha} \tag{4}$$

In this case, with L, M, ρ_s and ρ_f specified, the three independent variables employed to determine the geometry of the folded sandwich plate are: υ_s, H/L and α.

2.2. ***Material specifications.*** The core and face sheets of the sandwich plates are taken to be 304 stainless steel with density $\rho_s = 8000\,\mathrm{kg/m^3}$. A piecewise function

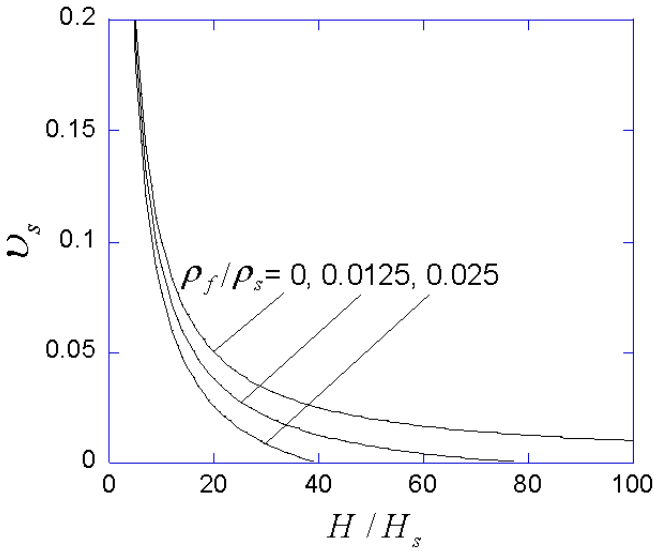

Figure 2: Volume fraction of steel versus normalized core thickness

has been fit to the true stress-log strain tensile behavior of the material giving

$$\sigma = \begin{cases} E_s\varepsilon & \varepsilon \le \sigma_{Ys}/E_s \\ \sigma_{Ys}(E_s\varepsilon/\sigma_{Ys})^N & \varepsilon > \sigma_{Ys}/E_s \end{cases} \tag{5}$$

with Young's modulus $E_s = 200$ GPa; Poisson's ratio $\nu = 0.3$; tensile yield strength $\sigma_{Ys} = 205$ MPa; strain hardening exponent $N = 0.17$ [American Society for Metals 1985]. The shear modulus and initial shear strength are $G_s = E_s/[2(1+\nu)] = 76.92$ GPa and $\tau_{Ys} = \sigma_{Ys}/\sqrt{3} = 118.35$ MPa. Strain-rate sensitivity of the steel is not taken into account. Classical flow theory based on the Mises yield surface and isotropic hardening is employed in the simulations. The steel is assumed sufficiently ductile to sustain large strains without fracture.

The constitutive model adopted for the foams is that developed for polymeric foams by [Zhang et al. 1997; Zhang et al. 1998] and available as a constitutive option in ABAQUS (Hibbit, Karlsson and Sorensen Inc., 2001a, 2001b). The model is an isotropic, dilatational plasticity relation. The specific form employed here models the inelastic deformation as perfectly plastic with three inputs: the yield stress in uniaxial compression, σ_c^0, the yield stress in hydrostatic compression, p_c^0, and the yield stress in hydrostatic tension, p_t^0. An ellipsoidal yield surface (see Figure 3) is specified by

$$\hat{\sigma} = \sigma_c^0 \tag{6}$$

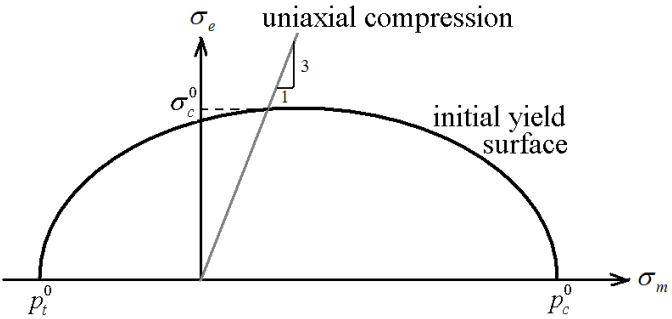

Figure 3: Initial yield surface for the continuum constitutive model of polymeric foam material

with $\hat{\sigma}$ as the *equivalent stress*, defined by

$$\hat{\sigma} \equiv \chi + \left[\chi^2 - 6\sigma_m \chi + \frac{\alpha^2 \sigma_m^2 + \sigma_e^2}{1 + (\alpha/3)^2}\right]^{1/2} \tag{7}$$

Here, $\sigma_e = \sqrt{3 s_{ij} s_{ij}/2}$ is the conventional effective stress with s_{ij} as the stress deviator, $\sigma_m = \sigma_{kk}/3$ is the mean stress,

$$\chi \equiv \frac{\alpha^2}{6\left[1 + (\alpha/3)^2\right]}(\sigma_c^0 - \sigma_t^0) \tag{8}$$

and the yield surface shape factor is

$$\alpha \equiv \frac{3\sigma_c^0/p_c^0}{\sqrt{(3p_t^0/p_c^0 + \sigma_c^0/p_c^0)(3 - \sigma_c^0/p_c^0)}} \tag{9}$$

Non-associative flow is assumed such that $\dot{\varepsilon}_{ij}^p \propto \partial G/\partial \sigma_{ij}$ with flow potential [Zhang et al. 1997; Zhang et al. 1998],

$$G = (\sigma_e^2 + 9\sigma_m^2/2)^{1/2} \tag{10}$$

Under uniaxial stressing, the model predicts that transverse plastic strains vanish, in approximate agreement with experimental findings of [Deshpande and Fleck 2001].

The formulation can incorporate strain hardening and, in particular, the substantial increase in flow stress associated with densification at large plastic compaction can be included. However, in the present application the strains are never large enough to cause significant strengthening due to densification, and the assumption of elastic-perfectly plastic behavior realistically captures the plateau-like response

Table 1: Mechanical properties of PVC polymeric foam

Foam	Young's modulus, E_f (MPa)	Poisson's ratio	Initial uniaxial compressive yield stress, σ_c^0 (MPa)	Initial hydrostatic compressive yield stress, p_c^0 (MPa)	Hydrostatic tensile yield stress, p_t^0 (MPa)
H100	105	0.2	1.1	1.0	1.8
H200	293	0.33	3.0	2.8	4.0

of the foam in the intermediate strain range. The formulation can also incorporate strain-rate dependence of the foam. Tests [Deshpande and Fleck 2001] in the range of strain-rates from $10^{-3}\,\mathrm{s}^{-1}$ to $10\,\mathrm{s}^{-1}$ reveal only a moderately weak rate dependence, which will be neglected in this first study.

Compression tests on the foam reveal some anisotropy with the yield strength typically about 20% higher in the rise direction of the foam than in transverse directions [Abot et al. 2002; Fleck and Sridhar 2002]. The isotropic model used here neglects this anisotropy; the uniaxial yield stress, σ_c^0, is associated with the direction perpendicular to the rise direction. The parameters characterizing the foam are presented in Table 1. The values for σ_c^0 and Young's modulus in Table 1 are taken from data in [Deshpande and Fleck 2001] and [Fleck and Sridhar 2002] and are lower than the values suggested by the manufacturer of the polymeric foams [DIAB Inc. $\geq$ 2006].

2.3. ***Finite element model and specification of the plates.*** The finite element models were developed using ABAQUS/CAE software. All components (face sheets, core webs and polymeric foam components) were fully meshed with three-dimensional elements. Eight-node brick elements were employed with reduced integration. The loading was taken to be independent of the coordinate in the long direction, and thus it was possible to analyze the three-dimensional unit of the plate that repeats periodically along its length as shown in Figure 1. Periodic boundary conditions were applied at each end of the repeating unit in the long direction, symmetry about the centerline was invoked, and clamped conditions were imposed along the two sides, corresponding to face sheets welded to rigid walls. Core webs were taken as welded to the face sheets. The commercial code, ABAQUS Explicit [Hibbit et al. 2001a], was utilized to perform most of the calculations, both dynamic and quasi-static.

Full-scale plates are considered in this paper whose half-width, L, is on the order of a meter. Steel sandwich plates with empty, square honeycomb cores optimized

against intense impulsive loads to have the minimum weight typically have a normalized core thickness $H/L \cong 0.3$ [Hutchinson and Xue 2005]. However, plates with $H/L = 0.1$ perform almost as well as the thicker optimal plates, and, because thinner cores are preferable in many applications, all the examples considered in this paper have $H/L = 0.1$. These optimal and near-optimal full-scale plates typically have between $1/5$ and $1/3$ of the their total mass in the core, corresponding to a volume fraction of core material in the range $0.02 < \upsilon_s < 0.05$. Several sets of calculations will be performed to explore the role of filling the core interstices with foam: (i) basic core responses to crush, shear and stretch; (ii) plate response to quasi-static load; and (iii) plate response to impulsive load.

3. Responses of empty and foam-filled cores subject to basic loading histories

The unit cells corresponding to core geometries of square honeycomb and folded plates are given in Figs. 4a and 4b, respectively, along with the coordinate system. To reveal the effect of filling the core interstices with foam, overall stress-strain curves of the core are computed using for three basic loading histories: core compression, in-plane tension and out-of-plane shear. These are the three most important loading histories for many applications.

The unit cells of Figure 4 are used in these finite element computations. In the compression and shear loadings, rigid plates are bonded to top and bottom surfaces of the unit cell to simulate the behavior of the core attached to the face sheets. The bottom plate is fixed and the top face is displaced. Periodicity is exploited, and periodic boundary conditions are imposed on the unit cell consistent with each loading. Thus, for example, in core compression of the square honeycomb the shear tractions on the web edges in Figure 4a are zero while the in-plane edge displacement parallel to the web is constrained to be zero, simulating overall uniaxial straining as constrained by the faces. For shear loading, there is no net force in the direction perpendicular to the faces. For the folded plate cell in Figure 4b, the length, ℓ, of the unit is a parameter that must be varied to determine the critical buckling mode. The loading referred to as in-plane tension is in reality overall tension subject to zero in-plane straining in the transverse direction consistent with stretching of the infinitely long plate clamped on its sides. For this loading, the edges of the web aligned with the direction of loading are displaced relative to one another uniformly while the edges of the transverse webs are constrained so they undergo no in-plane displacement parallel to the web. Shear tractions vanish on all the edges, and zero traction on the top and bottom edges is enforced in the direction perpendicular to the faces. Further details are described for the analogous calculations for empty cores in [Xue and Hutchinson 2004b]. In the finite element models of foam-filled cores, the displacements of the steel core and polymeric

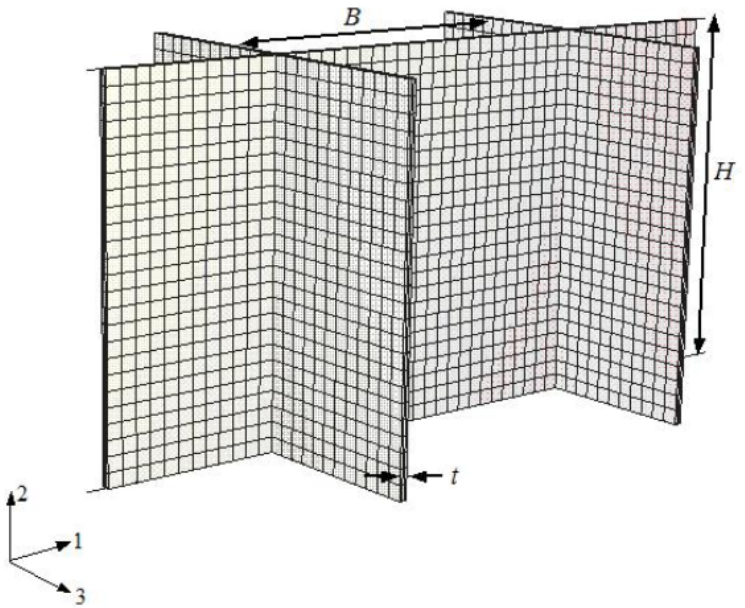

(a) Square honeycomb core geometry

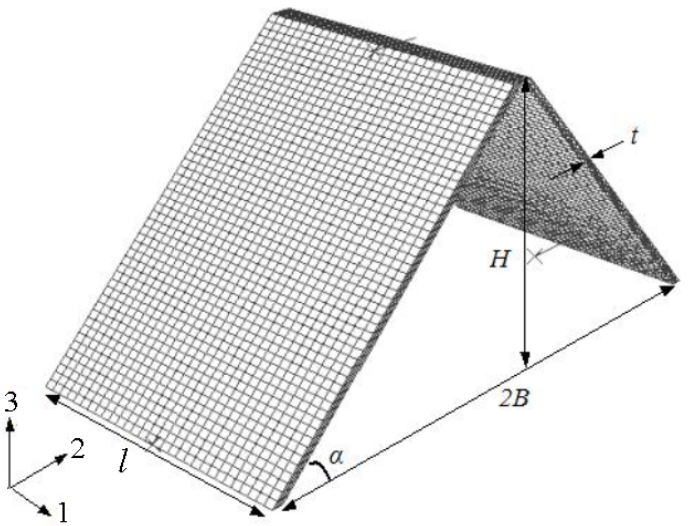

(b) Folded core geometry

Figure 4: Finite element model of a unit core cell

foam coincide at nodal points on shared interfaces. When analyzed with implicit methods, the problems addressed in this paper have very low rates of convergence, because of the complexity of the geometry and the extreme variation of the material behavior. For this reason, ABAQUS Explicit [Hibbit et al. 2001a] is utilized to simulate each simple stress history of empty and foam-filled cores. The analyses are performed under a sufficiently low rate of loading such that inertial effects are very small and the response is essentially quasi-static. Further discussion on this topic is presented in Section 4. The detailed analysis of the "micro" behavior of the core accounts for finite rotations and large plastic strains and it captures features such as plastic buckling and local necking of the core webs (square honeycomb) or core plate (folded sandwich).

3.1. ***Square honeycomb core.*** The overall stress-strain responses for the three basic loading histories are shown (Fig. 5) for a square honeycomb core with $H/B = 1$ and $t/B = 0.02$, corresponding to a volume fraction of steel, $\upsilon_s = 0.04$, whether empty or filled. The foam constitutes *additional* mass in this plot. The dimensions of the core are such that yielding occurs prior to elastic buckling, and plastic buckling is the source of nonlinear deformation for crushing and shearing. The stresses are defined as true stresses. The overall stresses, $\bar{\sigma}_{ij}$, are normalized by their initial yield values for the empty core given later. Because of its relevance to core crush, the compression history is determined to larger strains than in-plane tension and out-of-plane shear. Representative web buckling deflections are included in Figure 5 for compression and shear.

Estimates of the elastic stiffness and initial yield strength of the core based on simple strength of materials formulas are informative as to the role of the foam. For the square honeycomb, estimates of the overall elastic moduli associated with uniaxial stressing in the three directions of orthotropy and out-of-plane shearing are

$$\begin{aligned} E_{22} &\approx \upsilon_s E_s + (1-\upsilon_s) E_f \\ E_{11} = E_{33} &\approx \frac{1}{2}\upsilon_s E_s + (1-\frac{1}{2}\upsilon_s) E_f \\ G_{12} = G_{23} &\approx \frac{1}{2}\upsilon_s G_s + (1-\frac{1}{2}\upsilon_s) G_f \end{aligned} \tag{11}$$

with no accounting for constraint from the faces. The associated average density of the core, $\bar{\rho}_c$, is given by (1). For a typical core with $\upsilon_s = 0.04$, filling with H100 foam increases $\bar{\rho}_c$ by 30%, E_{22} by 1%, and E_{22} and G_{12} by 2%. The corresponding increases for H200 foam are roughly 60%, 3% and 6%. Obviously, the purpose of filling the core with foam is *not* to increase the overall elastic stiffness—employing the additional mass, as steel would be far more effective.

The effect of filling the core with foam on plastic yielding of the core *in the absence of buckling* is more significant than its effect on elastic stiffness. Two

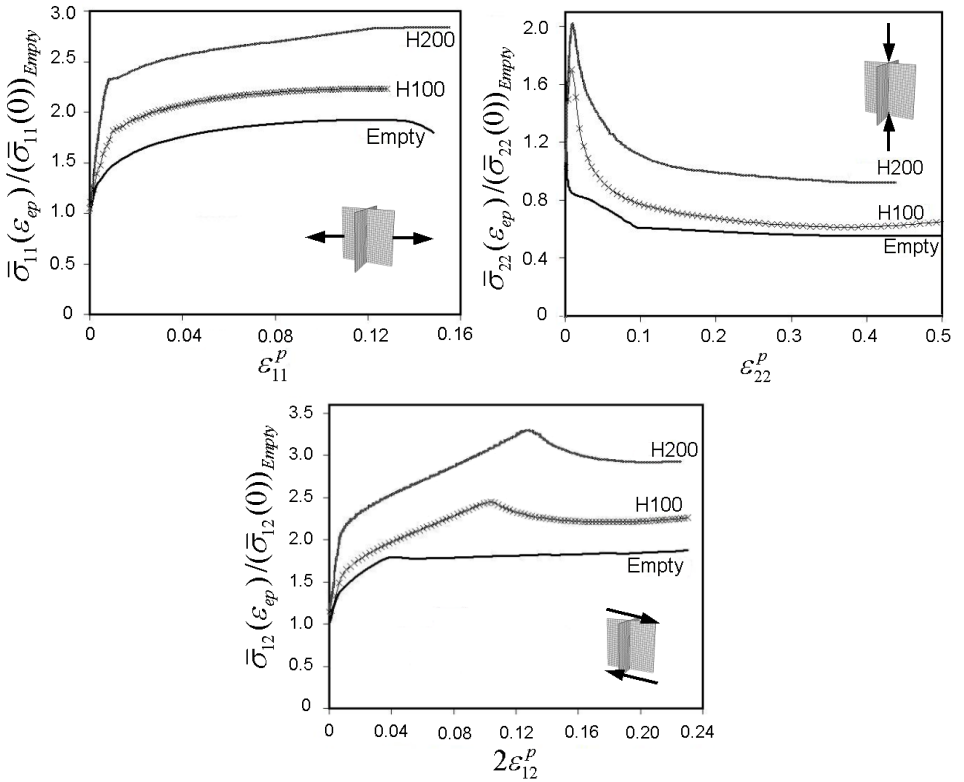

(a) Normalized true stress-true plastic strain relationships for each of the three basic histories for the square honeycomb core with $H/B = 1$ and $t/B = 0.02$ corresponding to $\upsilon_s = 0.04$ (ε_{ij}^{p} is the true plastic strain associated with the loading).

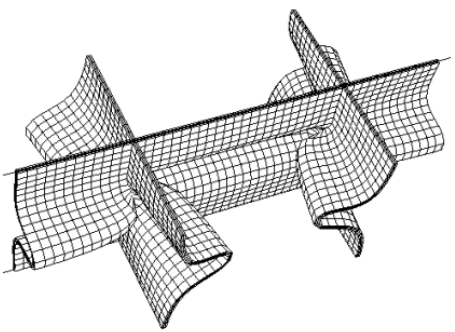

(b) Deformed configuration of the mesh showing compressive buckling of the web for empty square honeycomb core

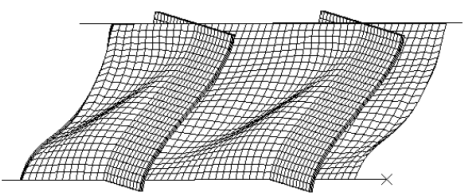

(c) Deformed configuration of the mesh showing shear buckling of the web for empty square honeycomb core

Figure 5

sets of estimates are given of the overall yield stress for uniaxial stressing in the directions of orthotropy (again with no constraint of the faces) and out-of-plane shearing: (i) the average stress at the strain when the steel yields and (ii) the average stress at the strain when the foam yields[1]. In uniaxial stressing, the steel yields at a strain of 0.1%, while the foams yield at a strain of about 1%. At the strain the steel yields:

$$\begin{aligned}
\bar{\sigma}_{22}(0) &\approx \upsilon_s \sigma_{Ys} + (1-\upsilon_s)(\sigma_{Ys}/E_s)E_f \\
\bar{\sigma}_{11}(0) = \bar{\sigma}_{33}(0) &\approx \frac{1}{2}\upsilon_s \sigma_{Ys} + (1-\frac{1}{2}\upsilon_s)(\sigma_{Ys}/E_s)E_f \\
\bar{\sigma}_{12}(0) = \bar{\sigma}_{23}(0) &\approx \frac{1}{2}\upsilon_s \tau_{Ys} + (1-\frac{1}{2}\upsilon_s)(\tau_{Ys}/G_s)G_f
\end{aligned} \tag{12}$$

Adding foam only increases the initial yield stresses by a few percent. The effect of the foam on the stress at the strain that the foam yields is more significant:

$$\begin{aligned}
\bar{\sigma}_{22} &\approx \upsilon_s \sigma_{Ys} + (1-\upsilon_s)\sigma_{Yf} \\
\bar{\sigma}_{11} = \bar{\sigma}_{33} &\approx \frac{1}{2}\upsilon_s \sigma_{Ys} + (1-\frac{1}{2}\upsilon_s)\sigma_{Yf} \\
\bar{\sigma}_{12} = \bar{\sigma}_{23} &\approx \frac{1}{2}\upsilon_s \tau_{Ys} + (1-\frac{1}{2}\upsilon_s)\tau_{Yf}
\end{aligned} \tag{13}$$

where the yield stresses of the foam are given in Table 1. Strictly, σ_{Ys} and τ_{Ys} should be identified with the corresponding yield strains of the foam, but the increase in stress in the steel above its initial yield due strain hardening at strains on the order of 1% is not large. The elevation in $\bar{\sigma}_{22}$ due to the H100 foam is almost 15% while that for the H200 foam is almost 40%. These increases are still only about half what would be achieved if extra mass were used to increase the steel in the webs. However, for in-plane stressing and out-of-plane shearing, H100 foam gives rise to an 30% increase in the overall yield stresses, while H200 foam increases them by about 80%. These increases are comparable to what would be achieved by increasing the steel in the webs rather filling with foam.

The effects noted above are clearly evident in the overall stress-strain curves in Figure 5. In these plots, each overall stress is normalized by the associated initial yield stress of empty core, $\bar{\sigma}_{ij}(0)_{empty}$, given by (12). First, consider in-plane tension in Figure 5. The overall strain range plotted is too small for necking to begin in the webs. The foam has almost no effect on first yield as expected from the results quoted above. However, the overall stress increases sharply for

[1] As in the case of overall elastic stiffness, these are based on elementary estimates from the strength of materials. They ignore, for example, lateral stresses that develop in uniaxial stressing due to difference in the Poisson ratios of the steel and the foam. Nevertheless, the simplicity of the formulas nicely reveals the role of the foam, and the formulas are sufficiently accurate for present purposes.

strains less than about 1% due to the fact that the foam is still elastic. The abrupt change in slope at a strain of about 1% denotes the point where the foam yields; the associated stress is given approximately by (13). For even larger strains, the increases in stress are due to strain hardening of the steel. The behavior in out-of-plane shear in Figure 5 is similar to that described for in-plane tension prior to web buckling which causes the drop in overall stress. Addition of the foam significantly delays the strain at which shear buckling occurs due to its constraint on the lateral deflection of the webs. The consequent effect is the significant increase in the overall flow strength of the core in shear. The foam also delays buckling of the webs in the compressive loading in Figure 5, although buckling occurs at much smaller plastic strains in compression. (The dimensions of the empty core are such that plastic yielding and elastic buckling are almost coincident in compression.) In the post-buckling range, foam helps to stabilize the webs resulting in higher overall stress. It remains to be seen in Section 4, whether the strengthening by the foam observed in Figure 5 will persist when foam is added with a corresponding reduction in steel.

3.2. ***Folded plate core.*** The folded plate core has full orthotropic anisotropy. In particular, the in-plane stretching stiffness and strength of the empty core are substantial in the 1-direction but negligible in the 3-direction. The core plate has core height H, core plate thickness t, and core inclination angle α. The width of the unit cell (Fig. 1b) is

$$B = t/\sin\alpha + H/\tan\alpha. \tag{14}$$

The volume fraction of the core occupied by steel, υ_s, and the relative density of the core, $\bar{\rho}_c$, can be obtained from (4) and (1), respectively.

In the calculations, two core geometries are considered: (a) $\alpha = 45°$ with $t/H = 0.0144$, corresponding to $B/H \approx 1.021$ and $\upsilon_s = 0.02$, and (b) $\alpha = 45°$ with $t/H = 0.0295$, corresponding to $B/H \approx 1.042$ and $\upsilon_s = 0.04$. In out-of-plane compression with no foam, core (a) buckles elastically prior to yielding, while core (b) yields plastically prior to buckling.

Simple estimates for the overall elastic moduli are

$$\begin{aligned}
E_{11} &\approx \upsilon_s E_s + (1-\upsilon_s)E_f \\
E_{22} &= \upsilon_s E_s \sin^4\alpha + (1-\upsilon_s)E_f \\
E_{33} &= (1-\upsilon_s)E_f \\
G_{12} &\approx \upsilon_s G_s \sin^2\alpha + (1-\upsilon_s)G_f \\
G_{23} &\approx \frac{1}{4}\upsilon_s E_s \sin^2 2\alpha + (1-\upsilon_s)G_f \\
G_{13} &\approx \frac{1}{2}\upsilon_s G_s \sin 2\alpha + (1-\upsilon_s)G_f
\end{aligned} \tag{15}$$

Terms of relative order t_c/H_c have been neglected. The overall stresses at which the steel yields (assuming no buckling of the webs) are,

$$\begin{aligned}
\bar{\sigma}_{11}(0) &\approx \sigma_{Ys}\left[\upsilon_s + (1-\upsilon_s)E_f/E_s\right] \\
\bar{\sigma}_{22}(0) &= \sigma_{Ys}\left[\upsilon_s \sin^2\alpha + (1-\upsilon_s)E_f/E_s\right] \\
\bar{\sigma}_{12}(0) &= \tau_{Ys}\left[\upsilon_s \sin\alpha + (1-\upsilon_s)G_f/G_s\right] \\
\bar{\sigma}_{23}(0) &= \tau_{Ys}\left[\upsilon_s \sin 2\alpha/2 + (1-\upsilon_s)G_f/G_s\right] \\
\bar{\sigma}_{13}(0) &= \tau_{Ys}\left[\upsilon_s \cos\alpha + (1-\upsilon_s)G_f/G_s\right]
\end{aligned} \tag{16}$$

The corresponding results for the overall stresses at the strain when the foam yields are

$$\begin{aligned}
\bar{\sigma}_{11} &\approx \upsilon_s\sigma_{Ys} + (1-\upsilon_s)\sigma_{Yf} \\
\bar{\sigma}_{22} &= \upsilon_s \sin^2\alpha\, \sigma_{Ys} + (1-\upsilon_s)\sigma_{Yf} \\
\bar{\sigma}_{12} &= \upsilon_s \sin\alpha\, \tau_{Ys} + (1-\upsilon_s)\tau_{Yf} \\
\bar{\sigma}_{23} &= \upsilon_s \sin 2\alpha\, \tau_{Ys}/2 + (1-\upsilon_s)\tau_{Yf} \\
\bar{\sigma}_{13} &= \upsilon_s \cos\alpha\, \tau_{Ys} + (1-\upsilon_s)\tau_{Yf} \\
\bar{\sigma}_{33} &= (1-\upsilon_s)\sigma_{Yf}
\end{aligned} \tag{17}$$

The basic stress histories for the folded plate core were computed by imposing periodicity conditions on the segment ends. The overall stress-strain curves for the three basic histories, each normalized by the associated initial yield stress of empty core, $\bar{\sigma}_{ij}(0)_{empty}$, are plotted in Figure 6 for the cores with $\upsilon_s = 0.02$ and in Figure 7 for $\upsilon_s = 0.04$. The response for shear, $\bar{\sigma}_{12}$, subsequent to buckling depends on the length of the segment, ℓ; the curves presented in Figs. 6 and 7 have $\ell/H = 1$; this choice ensures that the overall shear at the onset of buckling is only slightly above the critical value.

The webs of the folded plate core with $\upsilon_s = 0.02$ in Figure 6 are sufficiently thin such that elastic buckling occurs prior the plastic yielding of the empty steel core under compression $\bar{\sigma}_{22}$; plastic yielding then occurs immediately after the onset of buckling causing the overall stress to fall dramatically. The role of the foam is substantially increasing the core strength at strains less than about 1%, prior to foam yield, is similar to that described for the square honeycomb core. The effect of the foam on the compressive behavior, $\bar{\sigma}_{22}$, of the core with more steel ($\upsilon_s = 0.04$) in Figure 7 is qualitatively similar in most details. As expected, the strengthening of the foam-filled core relative to the empty core is greatest for the core with the lesser amount of steel.

The effect of the foam on the behaviors under in-plane tension and out-of-plane shear is in accord with the behavior of the square honeycomb cores. In the two

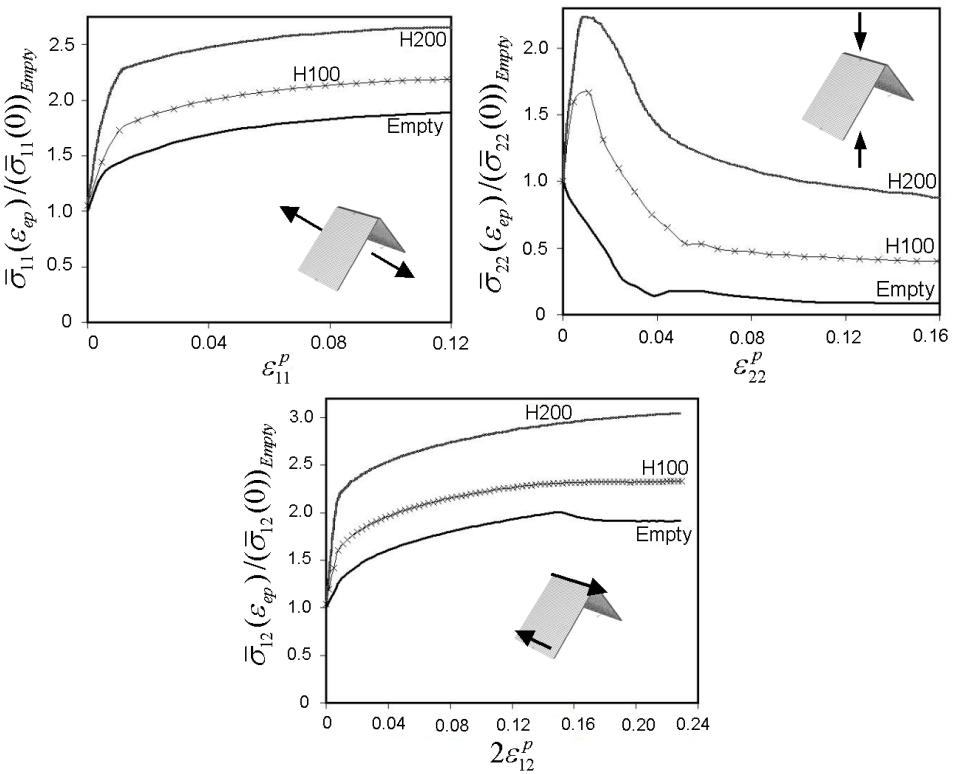

Figure 6: Normalized true stress-true plastic strain relationships for each of the three basic histories for the folded core with $\alpha = 45°$, $t/H = 0.0144$, corresponding to $\upsilon_s = 0.02$.

examples in Figs. 6 and 7, the foam effectively suppresses buckling in shear over the range of shear strain shown.

4. Empty and foam-filled sandwich plates under quasi-static loads

The objective of this section is to provide examples illustrating the influence of filling the core interstices on the structural performance of the two types of sandwich plates under conditions when the loading is quasi-static. Infinitely long plates of width $2L$, clamped along both sides, are subject to normal loads that are independent of the coordinate parallel to the sides. Both punch loads (see Figs. 8 and 9) and uniform pressure loads have been considered. However, because the findings related to the influence of the foam are similar for the two loading cases, only results for the punch load will be presented. Periodicity of the solution in the coordinate parallel to the edges permits analysis of sections of the plates shown in

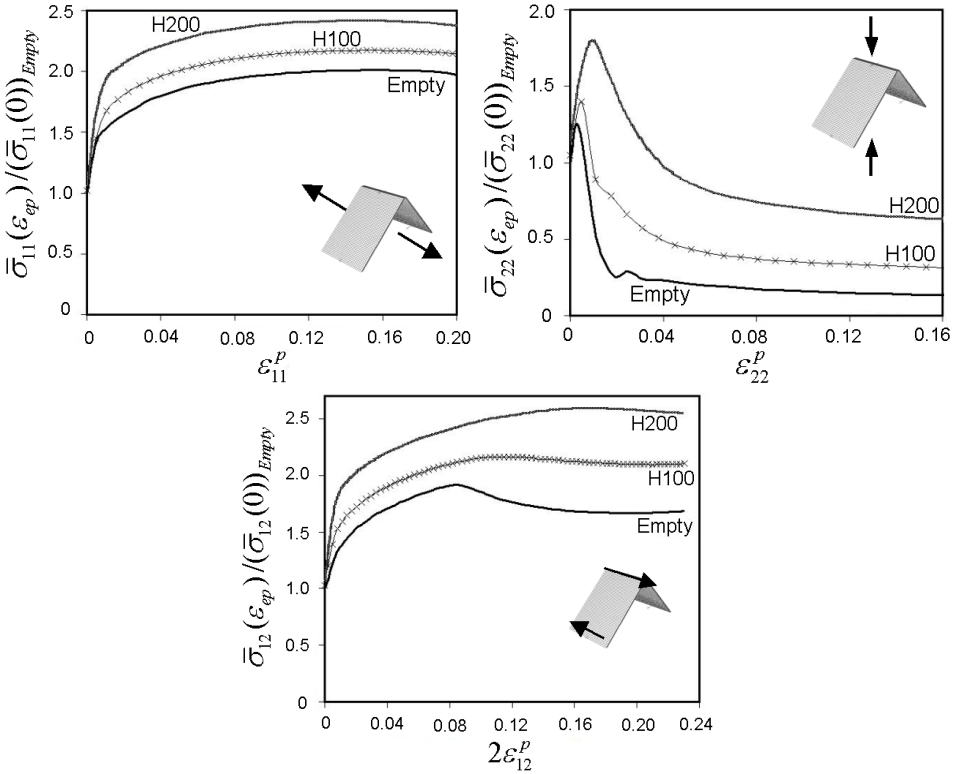

Figure 7: Normalized true stress-true plastic strain relationships for each of the three basic histories for the folded core with $\alpha = 45°$, $t/H = 0.0295$, corresponding to $\upsilon_s = 0.04$.

Figs. 8 and 9. Boundary conditions on the sections are imposed consistent with periodicity and symmetry. The three plates in each of these figures (empty core, core filled with H100, and core filled with H200) all have the same total mass. The amount of steel in the core is also the same for each of these plates; thus, the face sheets of the foam-filled plates have been thinned to offset the mass of the foam. (Alternative accommodation of foam mass by reducing the steel in the core will be considered in another example discussed later.)

For the finite element computations, the sections shown in Figs. 8 and 9 are fully meshed using the same types of three-dimensional elements described in Section 3. The computations are again carried out using ABAQUS Explicit with loads increased at a sufficiently low rate such that the response is effectively quasi-static. For the empty square honeycomb sandwich, the response of the sandwich plate so computed is compared with the result of computations performed using ABAQUS

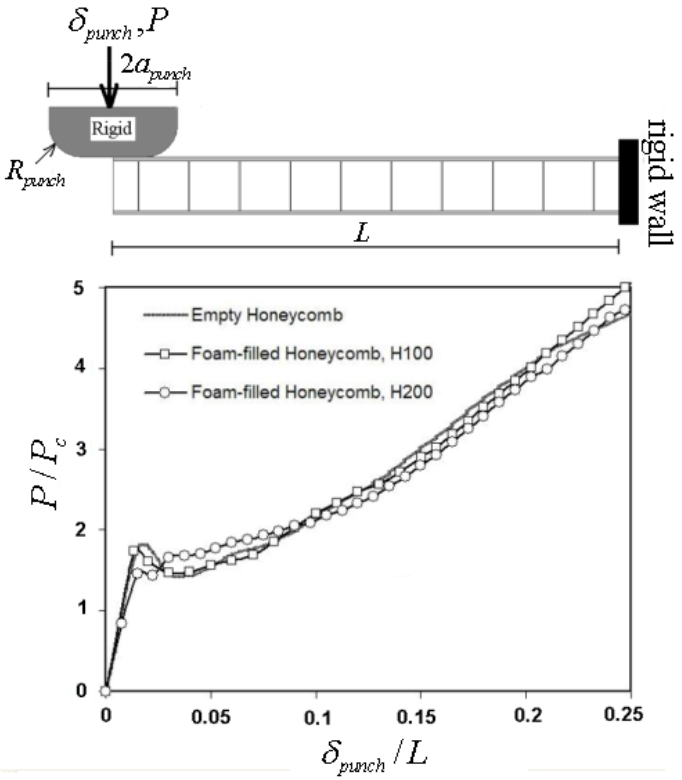

(a) The responses of clamped empty and foam-filled square honeycomb sandwich plates subject to quasi-static punch load

Figure 8
(continued on next page)

Standard [Hibbit et al. 2001b], and good agreement between the two sets of results is revealed. The load/length, P, in Figs. 8 and 9 is normalized by the limit load/length, P_c, for a perfectly plastic empty sandwich plate having limit bending moment/length, $4\sigma_{Ys}h_{face}H$ (based only on contributions from the faces), i.e.

$$P_c = 4\sigma_{Ys}h_{face}H/L \tag{18}$$

The main conclusion that emerges from the results in Figs. 8 and 9 is that there is remarkably little difference between the overall load-deflection behaviors of the sandwich plates with empty cores and that of the plates whose cores are filled with foam. However, there are differences in the details of the deformation. In particular, it can be noted from the deformed configurations shown in the lower

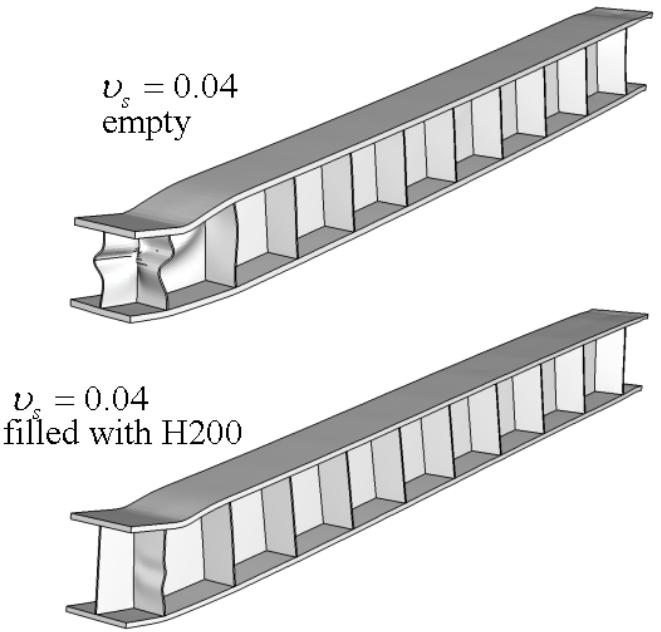

(b) Deformed configuration of the empty and foam-filled square honeycomb sandwich plate at $\delta_{punch}/L = 0.25$ (the polymeric foam components are not shown)

Figure 8 (cont.): The rigid punch is infinite in the direction perpendicular to the cross-section shown and has normalized half-width of $a_{punch}/L = 0.127$ and normalized edge radius of $R_{punch}/a_{punch} = 0.5$. All sandwich plates have $\bar{M}/(\rho_s L) = 0.02$, $H/L = 0.1$ and $B/H = 1$ and $\upsilon_s = 0.04$.

portion of Figs. 8 and 9 that the foam noticeably reduces the buckling deflection of the core webs beneath the indenter.

At low loads, bending dominates the behavior of the plate such that in-plane compressive stresses exist in the top face sheet and in-plane tensile stresses in the bottom face sheet. Plastic yielding begins at $\delta_{Punch}/L \cong 0.01$. Then, as deformation proceeds, the stresses on the top face sheet gradually change from compression to tension signaling the transition to stretching dominated behavior. For the sandwich plate configurations studied here, stretching takes over when δ_{Punch}/L exceeds 0.1. The foam enhances the core crushing strength by providing lateral support of the core webs, and, in this way, it influences the local response of the plate under the punch load. The energy absorbed by plastic deformation by the steel core beneath the indenter is significantly lower for the case of foam-filled sandwich

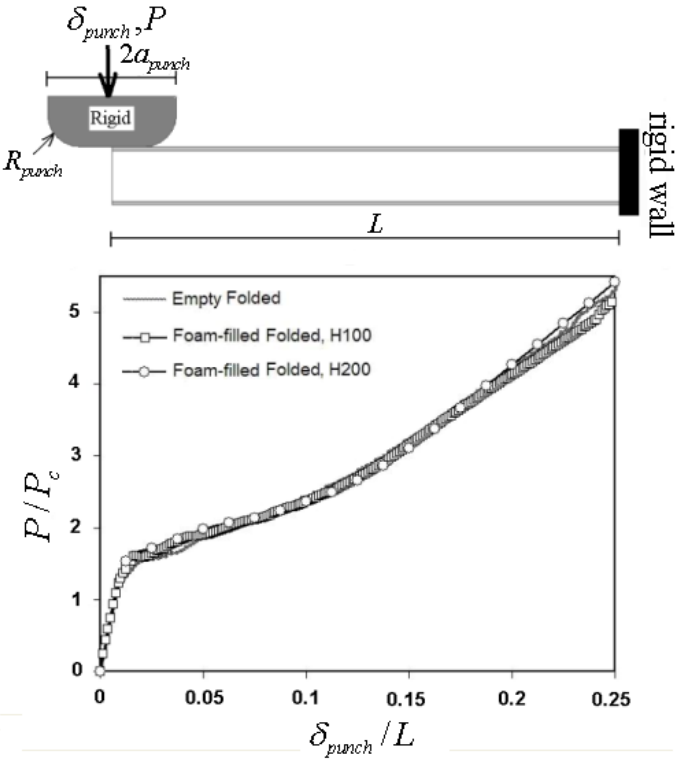

(a) The responses of clamped empty and foam-filled folded sandwich plates subject to quasi-static punch load

Figure 9
(continued on next page)

plates than for the empty core plates because the crushing is much less. In addition, by spreading the deformation more uniformly in the vicinity of the indenter, the foam-filled core may help reduce the tensile strains in the upper face sheet thereby suppressing, or delaying, necking.

5. Empty and foam-filled sandwich plates under impulsive loads

To simulate the response of the plates subject to a uniform air blast, a uniform impulse/area, I (Ns/m^2), is applied to the face sheet towards the blast at time $t = 0$ as a uniform initial velocity, $v = I/\rho_s h_{face}$. The rationale for replacing the pressure pulse by an initial impulse is based on the fact that the response time

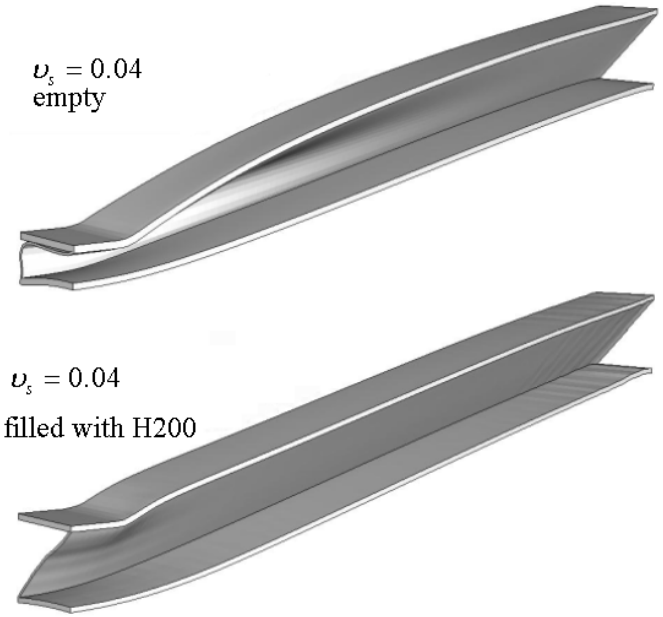

(b) Deformed configuration of the empty and foam-filled sandwich plate at $\delta_{punch}/L = 0.25$ (the polymeric foam components are not shown).

Figure 9 (cont.): The rigid punch is infinite in the direction perpendicular to the cross-section shown and has normalized half-width of $a_{punch}/L = 0.127$ and normalized edge radius of $R_{punch}/a_{punch} = 0.5$. All sandwich plates have $\bar{M}/(\rho_s L) = 0.02$, $\alpha = 45°$, $H/L = 0.1$ and $\upsilon_s = 0.04$.

associated with the overall deflection of the plate is large compared to the period of the pulse [Xue and Hutchinson 2003; Xue and Hutchinson 2004a; Fleck and Deshpande 2004]. For a full-scale plate, the dominant action of the pulse ceases before the face toward the blast has moved only several centimeters.

In this section, the responses of foam-filled square honeycomb and folded plate core sandwich plates under impulsive loads are compared to the corresponding responses of plates with unfilled cores. The plates are similar to those considered in the previous section: infinitely long, of width $2L$, and clamped along their edges. Results for both the deflection of the face sheet toward the blast and the core crushing strain are presented, as are selected results on energy dissipation within the sandwich plate. Define the average crushing strain of the core at the center of the plate by $\bar{\varepsilon}_c = \Delta H/H$, where ΔH is the reduction in core height. Denote

the final deflection at the center of the top face sheet by plate by δ. For the plate with the empty square honeycomb core, δ/L and $\bar{\varepsilon}_c$ depend on the following set of dimensionless parameters [Xue and Hutchinson 2004a]:

$$\frac{I}{M\sqrt{\sigma_{Ys}/\rho_s}},\ \frac{M}{\rho_s L},\ \upsilon_s,\ \frac{H}{L},\ \frac{B}{H}$$

plus N and σ_{Ys}/E. For plates with unfilled folded plate cores, normalized maximum deflection and the crushing strain at the center depend on the same list of dimensionless variables with the exception that B/H is replaced by α. In addition, dimensionless time variable governing the time-dependence is $t\Big/\left(L/\sqrt{\sigma_{Ys}/\rho_s}\right)$. The computations were carried out using ABAQUS Explicit with the same periodic sections and three-dimensional meshes introduced for the quasi-static loadings.

The effect of the momentum impulse imparted to the top face sheet of the sandwich plates, $I\Big/\left(M\sqrt{\sigma_{Ys}/\rho_s}\right)$, on δ/L and $\bar{\varepsilon}_c$ are presented in Figs. 10 and 11. Results for empty cores and foam-filled cores are shown. The plates in these figures all have the same total mass; foam mass is offset by thinning the face sheets, not the core webs. All the sandwich plates have $M/\rho_s L = 0.02$, $\upsilon_s = 0.04$, $H/L = 0.1$. For plates with honeycomb cores in Figure 10, $B/H = 1$, while for plates with folded plate cores in Figure 11, $\alpha = 45°$. The range of normalized impulse plotted covers the full range of realistic deflections. As was the case noted for the quasi-static loadings, there is remarkably little difference in the maximum top face deflection of the two classes of plates between the filled and unfilled cores. Foam reduces the crushing strain of the folded plate core (Figure 11), but this does not translate into a decrease in the overall deflection relative to the plate with the empty core. Inserting foam has little effect on the maximum crushing strain of plates with the square honeycomb cores. This is primarily due to the fact that the webs of the core are stabilized against buckling by their lateral inertia at the high crushing velocities considered here [Vaughn et al. 2005].

In studying the comparative advantages of equal weight filled and unfilled plates, one would obviously want to know whether it is best to offset the weight of the foam by thinning the face sheets or by thinning the core webs, or some combination of the two. We have not carried out a thorough optimization addressing this issue, but we will present one set of computations for the sandwich plates with the square honeycomb cores that provides some insight into the question. The dimensions of the unfilled sandwich plate in Figure 10 were established to be nearly optimal at a normalized impulse level of $I\Big/\left(M\sqrt{\sigma_{Ys}/\rho_s}\right) = 0.25$ by [Xue and Hutchinson 2004a]. In particular, the ratio of steel in the core to the total steel in the plate (20%) was found to minimize δ/L at that impulse level for all plates with the same total mass with $B/H = 1$ and $H/L = 0.1$. Moreover, the dependence on B/H and H/L was found to be relatively weak.

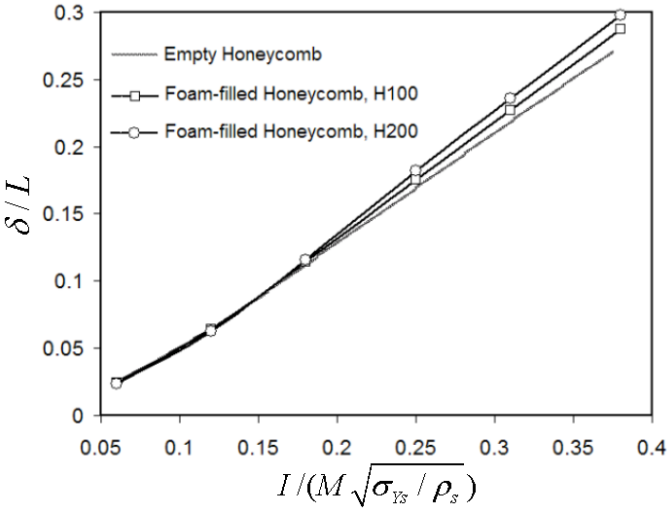

(a) The normalized maximum deflection of the top face sheet δ/L

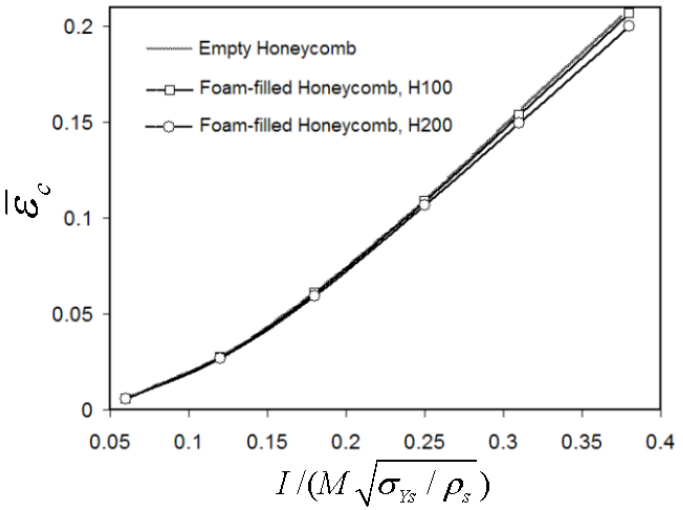

(b) The maximum nominal compressive strain in the core, $\bar{\varepsilon}_c$, of empty and foam-filled square honeycomb sandwich plates versus normalized momentum impulse, $I/\left(M\sqrt{\sigma_{Ys}/\rho_s}\right)$.

Figure 10: All sandwich plates have $\bar{M}/(\rho_s L) = 0.02$, $H/L = 0.1$ and $B/H = 1$ and $\upsilon_s = 0.04$.

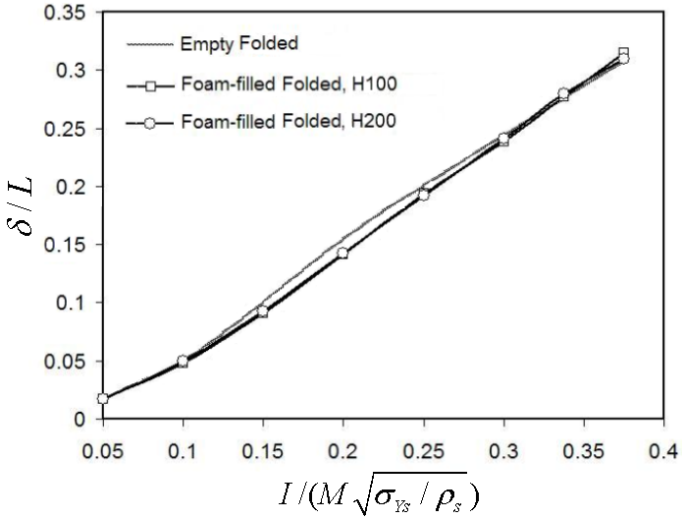

(a) The normalized maximum deflection of the top face sheet δ/L

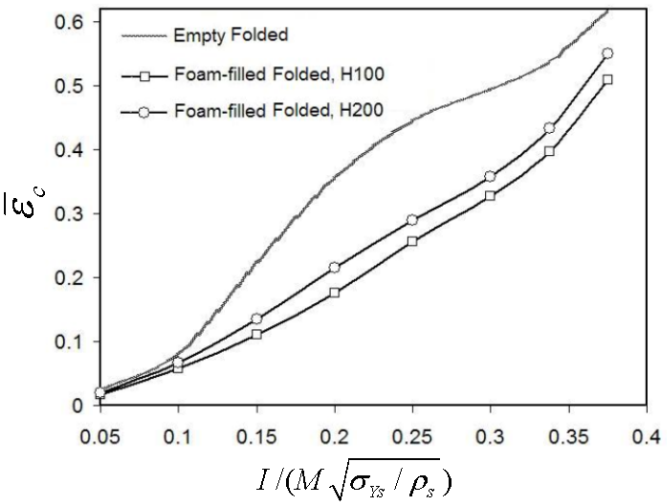

(b) The maximum nominal compressive strain in the core, $\bar{\varepsilon}_c$, of empty and foam-filled sandwich plates versus normalized momentum impulse, $I/\left(M\sqrt{\sigma_{Ys}/\rho_s}\right)$.

Figure 11: All sandwich plates have $\bar{M}/(\rho_s L) = 0.02$, $\alpha = 45°$, $H/L = 0.1$ and $\upsilon_s = 0.04$.

For the sandwich plates with the square honeycomb cores subject to an impulse, $I/\left(M\sqrt{\sigma_{Ys}/\rho_s}\right) = 0.25$, Figure 12 displays the dependence of the normalized maximum deflection, δ/L and the maximum core crushing strain on the volume fraction of steel in the core, υ_s, for unfilled cores and for cores filled with the two densities of foam. The total mass/area of each plate is the same with $M/\rho_s L = 0.02$; the deflection of the solid plate with the same mass/area and subject to the same impulse is included on the abscissa. Reducing ν_s increases the thickness of the faces and vise versa, because the mass of foam in the core varies only slightly over the range plotted of ν_s for each of the two foam-filled sandwiches. Thus, Figure 12 displays the tradeoff between core mass and face sheet mass. While the unfilled sandwich plate has the minimum deflection for cores with steel webs with relative density $\upsilon_s = 0.04$, the best performance from plates with foam-filled cores is achieved with lower relative density of steel—about 0.03 for the H200 foam. For plates with $\upsilon_s \geq 0.02$, the crushing strain is essentially the same for the filled and unfilled plates at the level of impulse imposed, and, moreover, it is less than 20%.

Figure 13 presents the final deformed configuration of the foam-filled square honeycomb sandwich plates (H200 Foam) for three volume fractions of the core occupied by steel, υ_s, under impulse, $I/\left(\bar{M}\sqrt{\sigma_{Ys}/\rho_s}\right) = 0.25$. As in the previous plots, all plates have $\bar{M}/(\rho_s L) = 0.02$, $H/L = 0.1$ and $B/H = 1$. For a low relative density of steel in the core ($\upsilon_s = 0.01$), local plastic buckling of the steel core clearly compromises the performance of the plate such that the crushing strain is almost 30%. For plates with excess steel in the core ($\upsilon_s = 0.08$) and therefore overly thinned face sheets, the top face undergoes extensive plastic bending into the core while the core webs undergo very little deformation. The intermediate case ($\upsilon_s = 0.04$) displays modest amounts of core deformation and face sheet bending. Note that for both $\upsilon_s = 0.04$ and $\upsilon_s = 0.08$, there is very little evidence of core web buckling, even though the core has been crushed to average strains of about 12% and 7%, respectively. These crushing strains are far in excess of the strain at plastic yield (a small fraction of 1%) and, also, well above the quasi-static plastic buckling strain of the webs. The suppression of buckling is due in part to the lateral support of the webs by the foam and the inertial stabilization of the webs under the impulsive loading.

A limited study on the effect of foam densification on the structural performance of square honeycomb sandwich plates filled with polymeric foam H200 under blast load is conducted by fitting a multi-linear line to the response of this material under uniaxial compressive load (see Section 2.2 for more detail). The sandwich plates having $\bar{M}/(\rho_s L) = 0.02$, $H/L = 0.1$ and $B/H = 1$ with various volume fractions of the core occupied by steel, $0 \leq \upsilon_s \leq 0.04$, are analyzed under the initial momentum $I/\left(\bar{M}\sqrt{\sigma_{Ys}/\rho_s}\right) = 0.25$. The result shows that the deformation mechanism

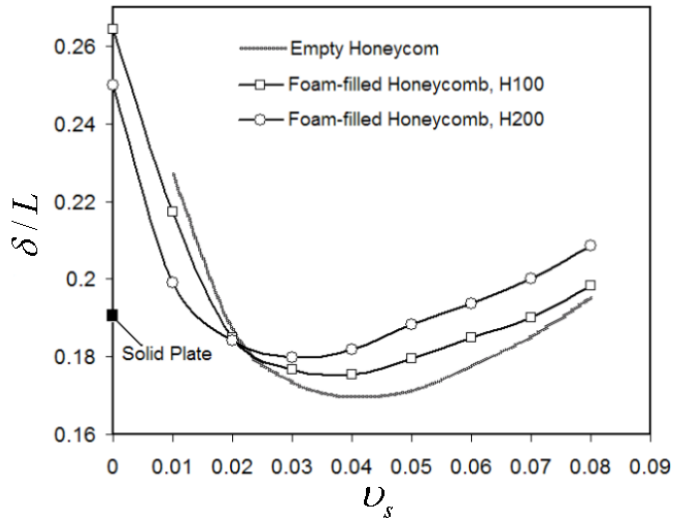

(a) The normalized maximum deflection of the top face sheet δ/L

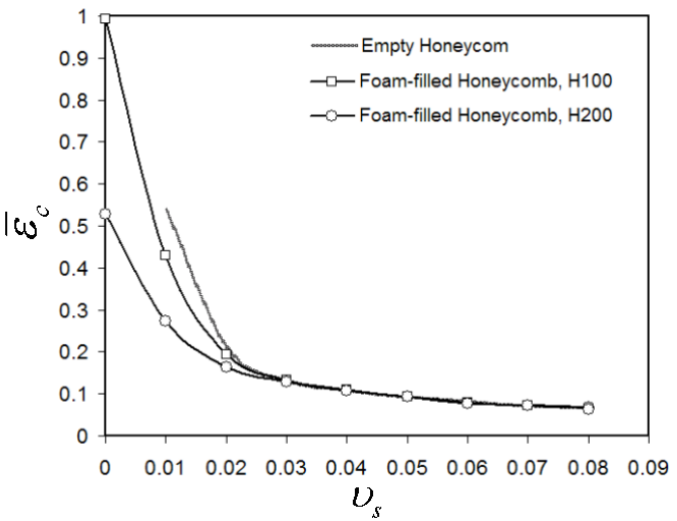

(b) The maximum nominal compressive strain in the core, $\bar{\varepsilon}_c$, of empty and foam-filled square honeycomb sandwich plates versus the volume fraction of the core occupied by steel, υ_s

Figure 12: All sandwich plates have $\bar{M}/(\rho_s L) = 0.02$, $H/L = 0.1$ and $B/H = 1$ and subjected to $I\Big/\left(M\sqrt{\sigma_{Ys}/\rho_s}\right) = 0.25$.

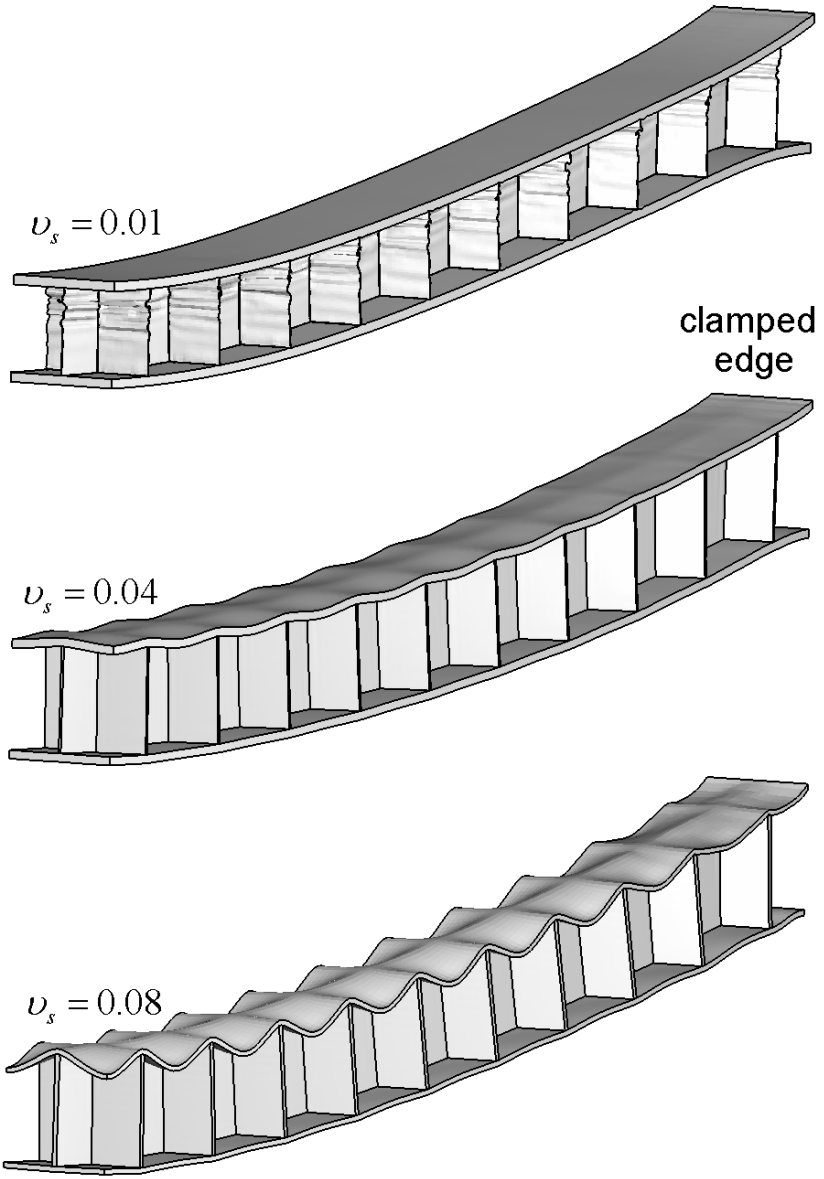

Figure 13: Deformed configurations of the foam-filled square honeycomb sandwich plates (H200 Polymeric Foam) for various volume fraction of the core occupied by steel, υ_s under the normalized momentum impulse $I\Big/\left(M\sqrt{\sigma_{Ys}/\rho_s}\right)=0.25$, at $t\Big/\left(\sqrt{\sigma_{Ys}/\rho_s}\right)=1$. All sandwich plates have $M/(\rho_s L)=0.02$, $H/L=0.1$ and $B/H=1$ (the polymeric foam components are not shown).

of the foam-filled square honeycomb sandwich plates is not significantly affected by considering the foam densification behavior under uniaxial compression. The maximum effect of accounting for foam densification on the maximum displacement of the top face sheet and maximum nominal compressive strain in the core are $\approx 1.1\%$ and $\approx 6.5\%$, respectively.

6. Plastic energy absorption in foam-filled honeycomb sandwich plates

Insight into the role of the polymer foam is gained by examining the contributions to plastic energy dissipation of each component of the empty and foam-filled (H200 foam) sandwich plates under impulsive load. Figure 14 displays the time history of the plastic dissipation in the core and face sheets along with the total plastic dissipation for the two plates, each of which has $M/\rho_s L = 0.02$, $\upsilon_s = 0.04$, $H/L = 0.1$, $B/H = 1$ and subject to $I\big/\big(\bar{M}\sqrt{\sigma_{Ys}/\rho_s}\big) = 0.25$. The results are plotted in dimensionless form as U_P/KE_0, where KE_0 is the initial kinetic energy imparted to the plate and U_P is the energy dissipated in plastic deformation in the component indicated at time $t\big/\big(L/\sqrt{\sigma_{Ys}/\rho_s}\big)$. The total dissipation is also shown.

For a prescribed initial momentum impulse applied to the top face sheet, I, the initial kinetic energies imparted to the plate is $KE_0 = I^2/(2\rho_s h_{face})$. Thus, the foam-filled plate has to absorb more energy than the unfilled plate since in the example in Figure 14 the face sheets of the filled plate are thinner than those of the unfilled plate (the total mass and the mass of steel in each core is the same for the two plates). The results in Figure 14 show that for both sandwich plates, the earliest stage of deformation with $t\big/\big(L/\sqrt{\sigma_{Ys}/\rho_s}\big) < 0.05$ (Stage II, [Fleck and Deshpande 2004]) consists of the top face sheet flying into, and crushing the core. In this stage, the motion away from the clamped supports is one-dimensional, the bottom face sheet is almost stationary, and very little plastic dissipation occurs in the bottom face sheets. By the end of this stage, the two face sheets are moving with nearly the same velocity. In this stage, the foam contributes significantly to the plastic energy dissipation of the foam-filled sandwich plate core layer by absorbing around 10% of the initial kinetic energy. As a consequence, the energy dissipated in the steel core of the foam-filled sandwich plate is around 10% smaller than that the empty sandwich one. The total plastic energy dissipated in the sandwich plate in stage II is almost the same for both cases ($\approx 60\%$), in close agreement with the simple analysis based on the conservation of momentum between the beginning and end of stage II [Fleck and Deshpande 2004].

Subsequent to stage II, there is essentially no further core compression and the entire sandwich plate undergoes bending followed by in-plane stretching (stage III of [Fleck and Deshpande 2004]. In this stage, the kinetic energy not absorbed in

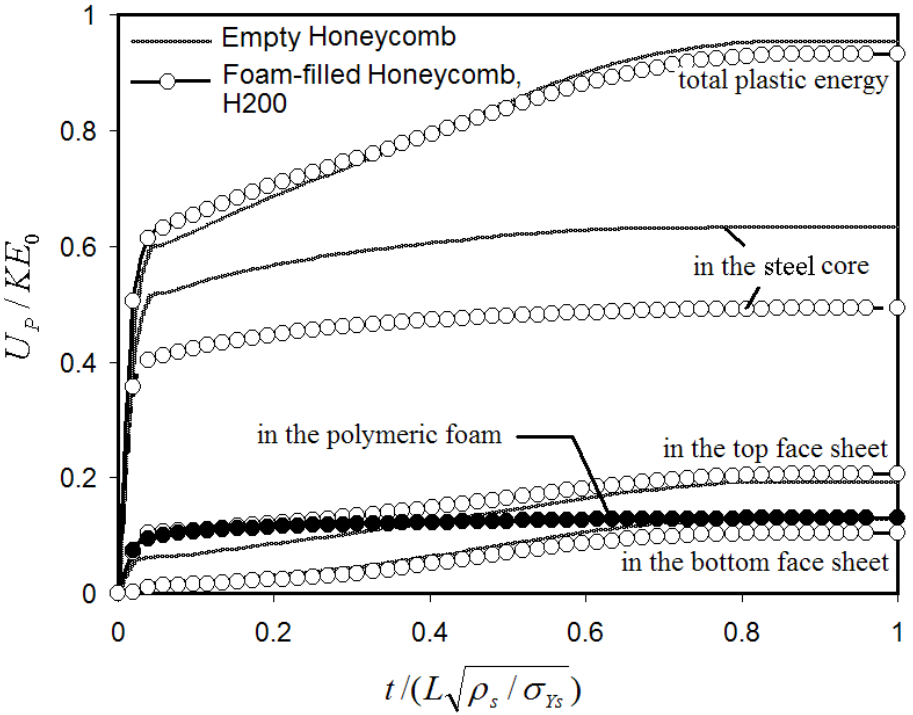

Figure 14: The time history of plastic dissipation in empty and foam-filled square honeycomb sandwich plates (H200 Polymeric Foam) with $M/(\rho_s L) = 0.02$, $\upsilon_s = 0.04$, $H/L = 0.1$ and $B/H = 1$ and subjected to $I\Big/\left(M\sqrt{\sigma_{Ys}/\rho_s}\right) = 0.25$.

core crush must be absorbed in overall bending and stretching. For both plates, almost all the plastic dissipation has occurred by $t\Big/\left(L/\sqrt{\sigma_{Ys}/\rho_s}\right) \approx 0.8$. Subsequently, the plate undergoes elastic vibration, although this is not evident in the plot of plastic energy dissipation. The total plastic energy dissipated in the empty and foam-filled sandwich plates is between 90% and 95% of the initial kinetic energy. The initial kinetic energy is never fully dissipated plastically because of residual elastic stress (the main contribution) and continuing elastic vibratory motion.

The influence of the relative density of the steel in the core, υ_s, on the energy dissipation in sandwich plate components for foam-filled (H200 foam) plates is seen in Figure 15. These plates all have the same total mass ($\bar{M}/(\rho_s L) = 0.02$, $H_c/L = 0.1$, $B/H_c = 0.1$), and thus increases in steel in the core is traded against steel in the faces in the same manner as the examples in Figure 12. The plates are all subject to $I\Big/\left(\bar{M}\sqrt{\sigma_{Ys}/\rho_s}\right) = 0.25$. The maximum plastic energy dissipated

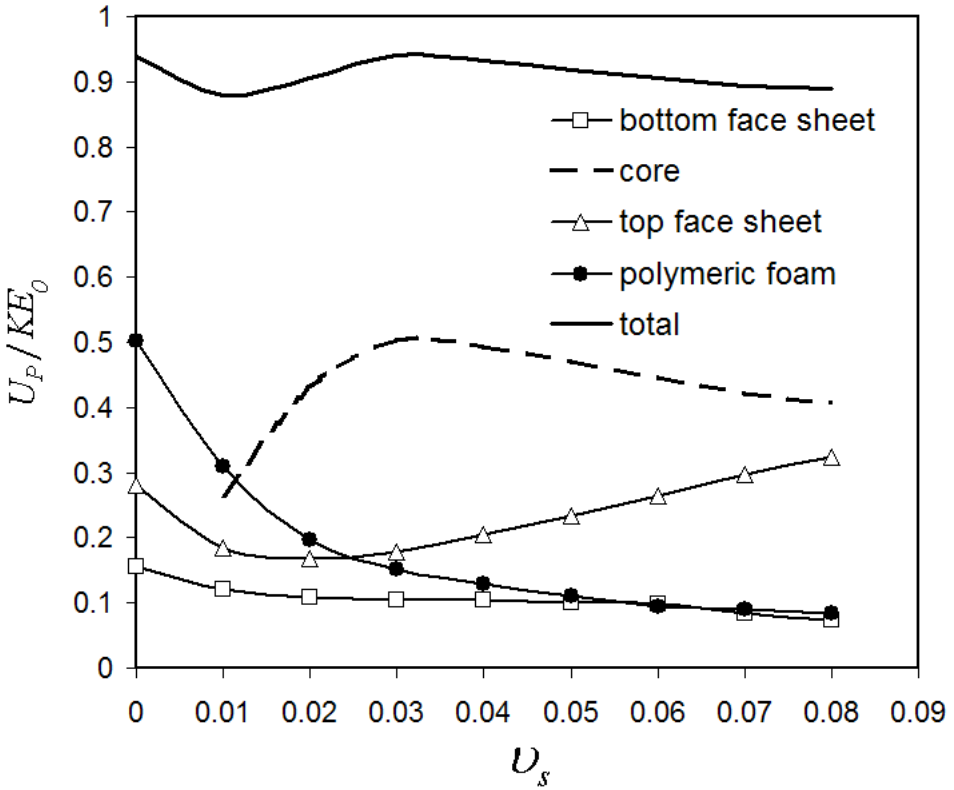

Figure 15: The plastic dissipation in foam-filled square honeycomb sandwich plates (H200 Polymeric Foam) versus the volume fraction of the core occupied by steel, υ_s, at $t\Big/\left(L/\sqrt{\sigma_{Ys}/\rho_s}\right) = 1$. All sandwich plates have $M/(\rho_s L) = 0.02$, $H/L = 0.1$, $B/H = 1$ and subjected to $I\Big/\left(M\sqrt{\sigma_{Ys}/\rho_s}\right) = 0.25$.

corresponds to $\upsilon_s = 0.03$, which is the configuration that experiences the minimum deflection (Figure 12). For the foam-filled plates with $\upsilon_s \geq 0.03$, the steel core can withstand the blast load without undergoing a significant plastic buckling (cf. Figure 13). For these sandwich plates, energy dissipation in the core occurs as compressive yielding of the steel core and polymeric foam. However, for smaller volume fractions of the core occupied by steel, $\upsilon_s < 0.03$, the steel webs undergo significant buckling and are unable to absorb energy as effectively as when they do not buckle.

7. Concluding remarks

The examples presented in this paper indicate that sandwich plates with foam-filled square honeycomb cores and folded plate cores exhibit comparable structural performance in resisting deformation to sandwich plates of equal mass with unfilled cores under representative quasi-static and impulsive loads. In other words, while there appears to be no clear advantage to filling the core with foam for structural purposes, there is no evident disadvantage either. Thus, if other compelling reasons to fill core interstices with foam exist, such as environmental protection or soundproofing, the examples here suggest that it should be possible to do this without structural penalty. These conclusions are drawn from the examples in the present study that have been limited to cores with thickness fixed relative to the half-width of the plate at $H/L = 0.1$. Earlier work has shown that this core thickness is associated with plates with near-optimal structural performance against uniformly distributed air and water blasts, although thicker cores can be somewhat more effective. Sandwich plates with foam-filled, thicker cores will have larger fraction of their total mass in foam, and it is not obvious that they will retain the structural performance of their unfilled counter parts. Thus, we emphasize that further study is required if sandwich plates have thickness significantly larger than $H/L = 0.1$.

Acknowledgement

This work has been supported in part by the ONR under grants GG10376-114934 and N00014–02–1–0700 and in part by the Division of Engineering and Applied Sciences, Harvard University.

References

[Abot et al. 2002] J. L. Abot, I. M. Daniel, and E. E. Gdoutos, "Contact Law for Composite Sandwich Beams", *Journal of Sandwich Structures and Materials* **4** (2002), 157–173.

[American Society for Metals 1985] B. H. E. and T. L. Gall (editors), *Metals Handbook Desk Edition*, American Society for Metals, 1985.

[Deshpande and Fleck 2001] V. S. Deshpande and N. A. Fleck, "Multi-Axial Yield Behavior of Polymer Foams", *Acta Materialia* **49** (2001), 1859–1866.

[DIAB Inc. $\geq$ 2006] DIAB Inc., "Divinycell Technical Manual, H Grade".

[Fleck and Deshpande 2004] N. A. Fleck and V. S. Deshpande, "Blast resistance of clamped sandwich beams", 2004. Submitted for publication to the *Journal of Applied Mechanics*.

[Fleck and Sridhar 2002] N. A. Fleck and I. Sridhar, "End Compression of Sandwich Columns", *Composites: Part A* **33** (2002), 353–359.

[Gibson and Ashby 1997] L. J. Gibson and M. F. Ashby, *Cellular Solids: Structures and properties*, Second ed., Cambridge University Press, Cambridge, 1997.

[Hibbit et al. 2001a] Hibbit, Karlsson, and Sorensen Inc., *ABAQUS/Explicit User's Manual, Version 6.0*, 2001.

[Hibbit et al. 2001b] Hibbit, Karlsson, and Sorensen Inc., *ABAQUS/Standard User's Manual, Version 6.0*, 2001.

[Hutchinson and Xue 2005] J. W. Hutchinson and Z. Xue, "Metal sandwich plates optimized for pressure impulses", *Int. J. Mech. Sci.* (2005). Article in press.

[Vaughn et al. 2005] D. Vaughn, M. Canning, and J. W. Hutchinson, "Coupled plastic wave propagation and column buckling", *J. Appl. Mech.* **72** (2005), 1–8.

[Xue and Hutchinson 2003] Z. Xue and J. W. Hutchinson, "Preliminary assessment of sandwich plates subject to blast loads", *Int. J. Mech. Sci.* **45** (2003), 687–705.

[Xue and Hutchinson 2004a] Z. Xue and J. W. Hutchinson, "A Comparative study of blast-resistant metal sandwich plates", *Int. J. Impact Engineering* **30** (2004), 1283–1305.

[Xue and Hutchinson 2004b] Z. Xue and J. W. Hutchinson, "Constitutive model for quasi-static deformation of metallic sandwich cores", *Int. J. Numerical Methods in Engineering* **61** (2004), 2205–2238.

[Zhang et al. 1997] J. Zhang, Z. Lin, A. Wong, N. Kikuchi, V. C. Li, A. F. Yee, and G. S. Nusholtz, "Constitutive Modeling and Material Characterization of Polymeric Foam", *Journal of Engineering Materials and Technology* **119** (1997), 284–291.

[Zhang et al. 1998] J. Zhang, N. Kikuchi, V. C. Li, A. F. Yee, and G. S. Nusholtz, "Constitutive Modeling of Polymeric Foam Material Subjected to Dynamic Crash Loading", *Int. J. Impact Engng.* **21** (1998), 369–386.

Received 9 May 05. Revised 7 Sep 05.

A. VAZIRI: *Division of Engineering and Applied Sciences, Harvard University, Cambridge MA 02138*
avaziri@deas.harvard.edu

Z. XUE: *Division of Engineering and Applied Sciences, Harvard University, Cambridge MA 02138*

J. W. HUTCHINSON: hutchinson@husm.harvard.edu
Division of Engineering and Applied Sciences, Harvard University, Cambridge MA 02138